Supporting Information

Structure-Constraint Induced Increase in Lewis Acidity of Tris(ortho-carboranyl)borane and Selective Complexation with Bestmann Ylides

Libo Xiang,[a,b] Junyi Wang,[c] Alexander Matler,[a,b] Qing Ye*[a,b]

[a] *Institute for Inorganic Chemistry, Julius-Maximilians-Universität Würzburg, Am Hubland, 97074 Würzburg (Germany)*

[b] *Institute for Sustainable Chemistry & Catalysis with Boron, Julius-Maximilians-Universität Würzburg, Am Hubland, 97074 Würzburg (Germany)*

[c] *Department of Chemistry*

Southern University of Science and Technology

518055 Shenzhen (P. R. China).

E-mail: qing.ye@uni-wuerzburg.de

Experimental procedures

General remarks

Unless otherwise noted, the following conditions apply.

All the manipulations were carried out using standard Schlenk lines or glovebox under an argon atmosphere. All the solvents were dried following standard techniques. C_6D_6 was distilled from Na/K and stored under an argon atmosphere before use. $CDCl_3$ was dried and stored over 4 molecular sieves before use. Ph_3PCCO was purchased from commercial sources and used without further purification. Cy_3PCCO [1], $LiC_2B_{10}H_{11}$ [2], $(C_2B_{10}H_{10})_2BBr$ [3a] and ^{Me}I*i*Pr [3b] were synthesized according to the literature. Other reagents were used as received without further purification.

The nuclear magnetic resonance spectroscopy was recorded on a Bruker Avance-400 (^1H 400.1 MHz; ^{11}B 128.5 MHz; ^{13}C 101 MHz; ^{31}P: 162. MHz) spectrometer at room temperature. ^{11}B NMR, $^{11}B\{^1H\}$ spectra were referenced relative to 15% $BF_3{\cdot}OEt_2$. $^{31}P\{^1H\}$ NMR chemical shifts are relative to 85% H_3PO_4. High-resolution mass spectrometry (HRMS) was performed with a Thermo Fisher Scientific Q-Exactive MS System. Elemental analysis (C, H, N) was performed on a vario micro cube CHNS analyzer. IR spectra were recorded on a Bruker FT-IR spectrometer ALPHA II inside a glovebox.

Synthesis and Spectral Data

Synthesis of 1

The 5 mL toluene solution of $(C_2B_{10}H_{10})_2BBr$ (375.1 mg, 1 mmol) was slowly added to a toluene (50 mL) suspension of $LiC_2B_{10}H_{11}$ (150.2 mg, 1 mmol) at –78 °C and warmed to room temperature gradually. The reaction mixture was stirred for 12 hours at room temperature. The suspension was filtrated to separate the lithium salt and all volatiles of the filtrate were removed under reduced pressure to obtain the product as a pale-yellow solid. The analytically pure product was crystallized from concentrated toluene solution at –30 °C for 12 h to yield **1** as a colorless crystalline solid.

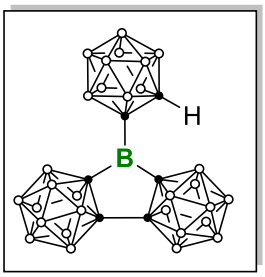

^{1}H NMR (400 MHz, C_6D_6): δ [ppm] = 3.68–1.42 (br. m, 30H, B*H*), 3.70 (s, 1H, $C_{carborane}$*H*). **^{1}H{^{11}B} NMR** (400 MHz, C_6D_6): δ [ppm] = 2.11 (s, 3H, B*H*), 2.28 (s, 5H, B*H*), 2.33 (s, 3H, B*H*), 2.45 (s, 3H, B*H*), 2.67 (s, 4H, B*H*), 2.76 (s, 4H, B*H*), 2.87 (s, 4H, B*H*), 2.98 (s, 1H, B*H*), 3.09 (s, 2H, B*H*), 3.20 (s, 1H, B*H*), 3.70 (s, 1H, $C_{carborane}$*H*). **^{11}B NMR** (128 MHz, C_6D_6): δ [ppm] = 65.22 (br, s, *B*–*o*-carborane), 5.64 (d. *J* = 153.3 Hz, $B_{carborane}$), –2.40 (d. *J* = 163.4 Hz, $B_{carborane}$), –5.51 (d. *J* = 153.3 Hz, $B_{carborane}$), –11.60 (d. *J* = 147.9 Hz, $B_{carborane}$). **^{11}B{^{1}H} NMR** (128 MHz, C_6D_6): δ [ppm] = 64.94 (br, s, *B*–*o*-carborane), 5.63 (s, $B_{carborane}$), -0.64 (s, $C_{carborane}$B), –2.43 (s, $B_{carborane}$), –5.42 (s, $B_{carborane}$), –7.33 (s, $B_{carborane}$), –11.54 (s, $B_{carborane}$). **^{13}C{^{1}H} NMR** (100 MHz, C_6D_6): δ [ppm] = 59.7 (s, $C_{carborane}$), 79.7 (s, $C_{carborane}$), **Elemental analysis**: calcd. for $C_6H_{31}B_{31}$, C, 16.44; H, 7.13; found C, 16.20; H, 6.22. **HRMS (LIFDI)**: calcd. for $C_6H_{31}B_{31}$ 438.5528; found: 438.5519. Yield: 64 % (279.9 mg, 0.64 mmol).

Synthetic protocols for 3

The 1 mL toluene solution of Bestmann's ylide R_3PCCO (0.32 mmol) was slowly added to a solution of **1** (106 mg, 0.32 mmol) in 5 mL toluene at room temperature. The reaction mixture was stirred for 4 h. The precipitate was collected through filtration and the remaining solid was dried under high vacuum to give the crude product as a white solid. The analytically pure product was crystallized from concentrated toluene solution at –30 °C for 12 h to yield **2** as a colorless crystalline solid.

For **3a:**

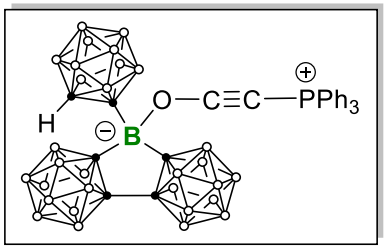

^{1}H NMR (400 MHz, C_6D_6): δ [ppm] = 2.02–3.98 (br. m, 30H, B*H*), 4.12 (s, 1H, $C_{carborane}$*H*), 6.88–6.92 (m, 6H, *H* of Ph), 6.94–6.97 (m, 3H, *H* of Ph), 7.17 to 7.23 (m, 6H, *H* of Ph). **^{1}H{^{11}B} NMR** (400 MHz, C_6D_6): δ [ppm] = 2.51 (s, 2H, B*H*), 2.62 (s, 2H, B*H*), 2.67 (s, 2H, B*H*), 2.73 (s, 4H, B*H*), 2.80 (s, 4H, B*H*), 2.90(s, 8H, B*H*), 3.10(s, 3H, B*H*), 3.19(s, 1H, B*H*), 3.25 (s, 2H, B*H*), 3.66 (s, 2H, B*H*), 4.12(s, 1H, $C_{carborane}$*H*), 6.88–6.92 (m, 6H, *H* of Ph), 6.95–6.97 (m, 3H, *H* of Ph), 7.18–7.23 (m, 6H, *H* of Ph). **^{11}B NMR** (128 MHz, C_6D_6): δ [ppm] = 0.65 (br, s, $B_{carborane}$), −3.64 (d. J = 153.7 Hz, $B_{carborane}$), −7.71 (br, s, $B_{carborane}$), −11.88 (br, s, $B_{carborane}$). **^{11}B{^{1}H} NMR** (128 MHz, C_6D_6): δ [ppm] = 0.80 (s, $B_{carborane}$), −3.53 (s, $C_{carborane}$B), −7.53 (s, $B_{carborane}$), −12.00 (s, $B_{carborane}$). **^{31}P{^{1}H} NMR** (162 MHz, C_6D_6): δ [ppm] = 5.17. **^{13}C{^{1}H} NMR** (100 MHz, C_6D_6): δ [ppm] = 13.30 (d, $J_{P\text{-}C}$ = 133 Hz, P=C), 60.6 (s, $C_{carborane}$), 78.5 (s, $C_{carborane}$), 121.3 (d, $J_{P\text{-}C}$ = 100.6 Hz. *C* of Ph), 128.6 (d, $J_{P\text{-}C}$ = 76.9 Hz. *C*O), 129.6 (d, $J_{P\text{-}C}$ = 13.8 Hz. *C* of Ph), 132.4 (d, $J_{P\text{-}C}$ = 12.3 Hz. *C* of Ph), 134.2 (d, $J_{P\text{-}C}$ = 3.2 Hz. *C* of Ph). **HRMS**: calcd. for $[C_{26}H_{46}B_{31}OP]^{+}$, 740.6389; found: 740.6497. Yield: 75 % (177.8 mg, 0.24 mmol). **IR**: 2198, 1603, 1439, 1112 cm^{-1}.

For **3b:**

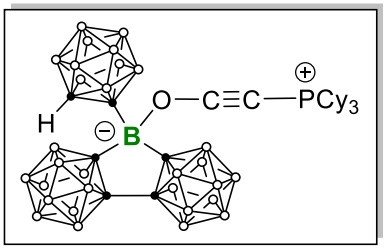

^{1}H NMR (400 MHz, $CDCl_3$): δ [ppm] = 1.32–1.38 (m, 10H, *H* of Cy), 1.54–1.57 (m, 6H, *H* of Cy), 3.30–3.67 (m, 47H, Cy and carborane overlaped), 3.96 (s, 1H, $C_{carborane}$*H*). **^{1}H{^{11}B} NMR** (400 MHz, $CDCl_3$): δ [ppm] = 1.33–1.39 (m, 10H, *H* of Cy), 1.54 to 1.57 (m, 6H, *H* of Cy), 1.85 (br, s, 3H, *H* of Cy), 1.98–2.02 (m, 14H, *H* of Cy), 2.12–2.24 (s, 15H, B*H*), 2.36 (s, 4H, B*H*), 2.40 (s, 4H, B*H*), 2.54 (s, 2H, B*H*), 2.62 (s, 2H, B*H*), 3.17 (s, 1H, B*H*), 3.29 (s, 2H, $C_{carborane}$*H*), 3.97 (s, 1H, $C_{carborane}$*H*). **^{11}B NMR** (128 MHz, $CDCl_3$): δ [ppm] = −0.36 (s, $B_{carborane}$), −4.30 (d, J = 148.8 Hz, $B_{carborane}$), −8.08 (br, s, $B_{carborane}$), −12.26 (br, s, $B_{carborane}$). **^{11}B{^{1}H} NMR** (128 MHz, $CDCl_3$): δ [ppm] = −0.29 (s, $B_{carborane}$), −4.17 (s, $B_{carborane}$), −8.16 (s, $B_{carborane}$), −12.52 (s, $B_{carborane}$). **^{31}P{^{1}H} NMR** (162 MHz, $CDCl_3$): δ [ppm] = 23.3. **^{13}C{^{1}H} NMR** (100 MHz, $CDCl_3$): δ [ppm] = 25.3 (d, $J_{P\text{-}C}$ = 1.6 Hz. *C* of Cy), 26.5 (d, $J_{P\text{-}C}$ = 13.2 Hz. *C* of Cy), 27.0 (d, $J_{P\text{-}C}$ = 3.5 Hz. *C* of Cy), 32.7 (d, $J_{P\text{-}C}$ = 51.6 Hz. *C* of Cy), 60.2 (s, $C_{carborane}$), 77.2 (s, $C_{carborane}$), 128.6 (d, $J_{P\text{-}C}$ = 81.9 Hz. *C*O). **HRMS**: calcd. for $[C_{26}B_{31}H_{63}OP]^{-}$, 757.7719; found: 757.7708. Yield: 82 % (197.0 mg, 0.26 mmol). **IR**: 2199, 1640, 1447, 1078 cm^{-1}.

Synthetic protocols for 4a

^{Me}I*i*Pr (5 mg, 0.027 mmol) was added to a toluene (1 mL) solution of **3a** (200 mg, 0.27 mmol) and

stirred at room temperature for 10 min. All volatiles were removed under reduced pressure to obtain a colorless solid. Colorless crystals were obtained by storing the saturated toluene solution of **4a** under −30 °C overnight.

For **4a:**

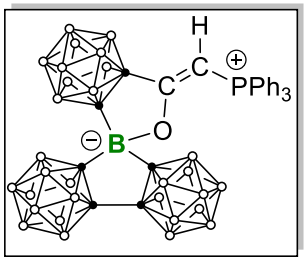

^{1}H NMR (400 MHz, C_6D_6): δ [ppm] = 2.01–3.76 (br. m, 30H, B*H*), 4.65 (d, 1H, $J_{P\text{-}C}$ = 12.9 Hz. C*H*), 6.92–6.94 (m, 6H, *H* of Ph), 6.95–6.99 (m, 6H, *H* of Ph), 7.03 to 7.08 (m, 3H, *H* of Ph). **^{1}H{^{11}B} NMR** (400 MHz, C_6D_6): δ [ppm] = 1.88 (s, 2H, B*H*), 2.55 (s, 4H, B*H*), 2.63 (s, 2H, B*H*), 2.72 (s, 4H, B*H*), 2.80 (s, 2H, B*H*), 2.87 (s, 2H, B*H*), 2.96 (s, 2H, B*H*), 3.05 (s, 8H, B*H*), 3.20 (s, 2H, B*H*), 3.46 (s, 2H, B*H*), 4.65 (d, 1H, $J_{P\text{-}C}$ = 13.0 Hz. C*H*), 6.88–6.92 (m, 6H, *H* of Ph), 6.95–6.97 (m, 3H, *H* of Ph), 7.18–7.23 (m, 6H, *H* of Ph). **^{11}B NMR** (128 MHz, C_6D_6): δ [ppm] = 2.69 (br, s, $B_{carborane}$), 0.49 (br, s, $B_{carborane}$), −3.74 (br, s, $B_{carborane}$), −7.52 (br, s, $B_{carborane}$), −10.85 (br, s, $B_{carborane}$). **^{11}B{^{1}H} NMR** (128 MHz, C_6D_6): δ [ppm] = 2.76 (s, $B_{carborane}$), 0.01 (s, $C_{carborane}$B), −4.50 (s, $B_{carborane}$), −6.98 (s, $B_{carborane}$). **^{31}P{^{1}H} NMR** (162 MHz, C_6D_6): δ [ppm] = 12.64. **^{13}C{^{1}H} NMR** (100 MHz, C_6D_6): δ [ppm] = 67.5 (s, $C_{carborane}$), 77.9 (s, $C_{carborane}$), 119.9 (d, $J_{P\text{-}C}$ = 95.6 Hz. *C* of Ph), 128.6 (d, $J_{P\text{-}C}$ = 75.4 Hz. *C*O), 129.9 (d, $J_{P\text{-}C}$ = 13.2 Hz. *C* of Ph), 132.8 (d, $J_{P\text{-}C}$ = 12.3 Hz. *C* of Ph), 134.3 (d, $J_{P\text{-}C}$ = 3.1 Hz. *C* of Ph). **HRMS**: calcd. for $[C_{26}H_{46}B_{31}OP]^+$, 740.6389; found: 740.6496. Yield: 82 % (163.1 mg, 0.22 mmol); **IR**: 2923, 1615, 1436, 1112 cm^{-1}.

NMR Spectroscopy

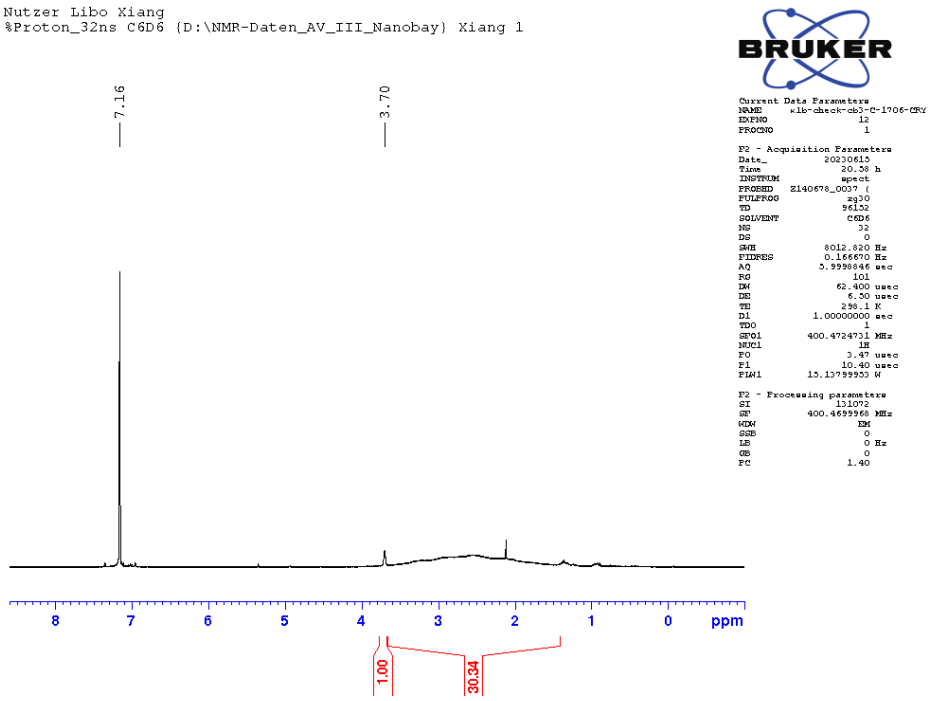

Figure S1. ^{1}H NMR spectrum of **1** in C_6D_6 at 298 K.

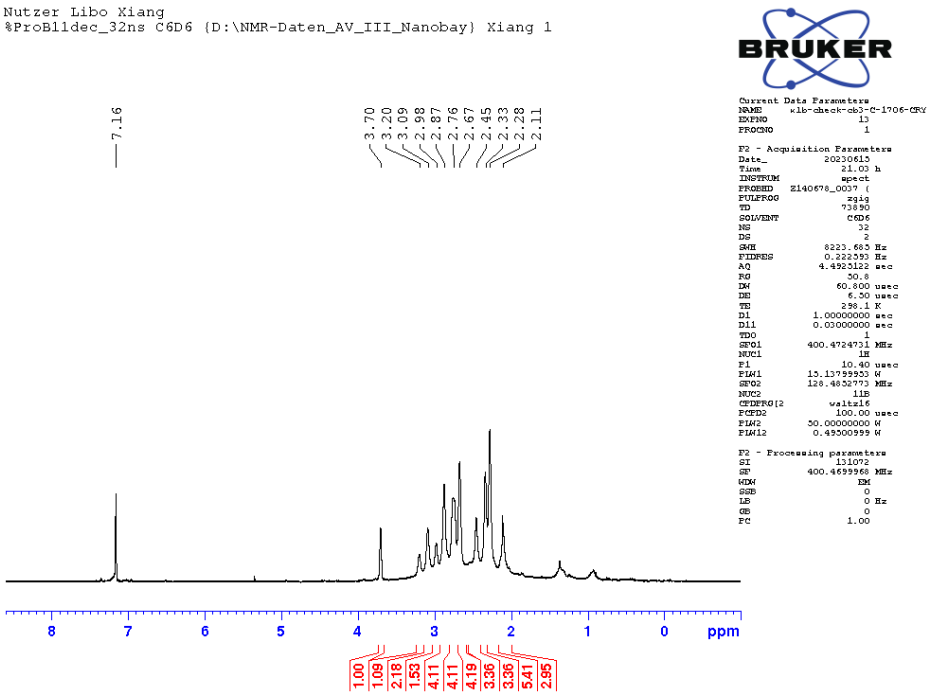

Figure S2. ^{1}H{^{11}B} NMR spectrum of **1** in C_6D_6 at 298 K.

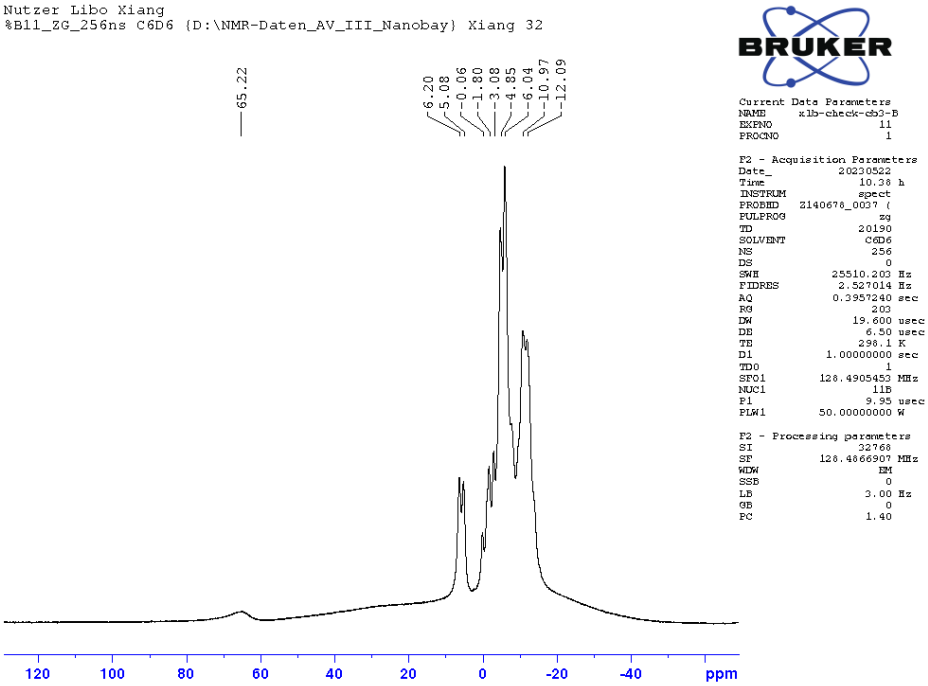

Figure S3. ^{11}B NMR spectrum of **1** in C_6D_6 at 298 K.

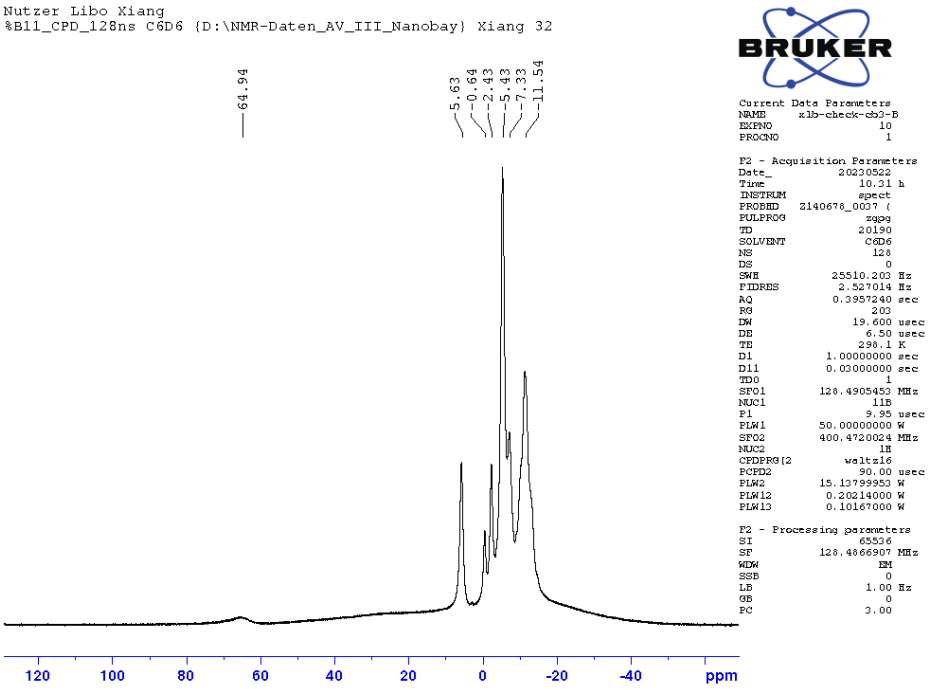

Figure S4. ^{11}B{^{1}H} NMR spectrum of **1** in C_6D_6 at 298 K.

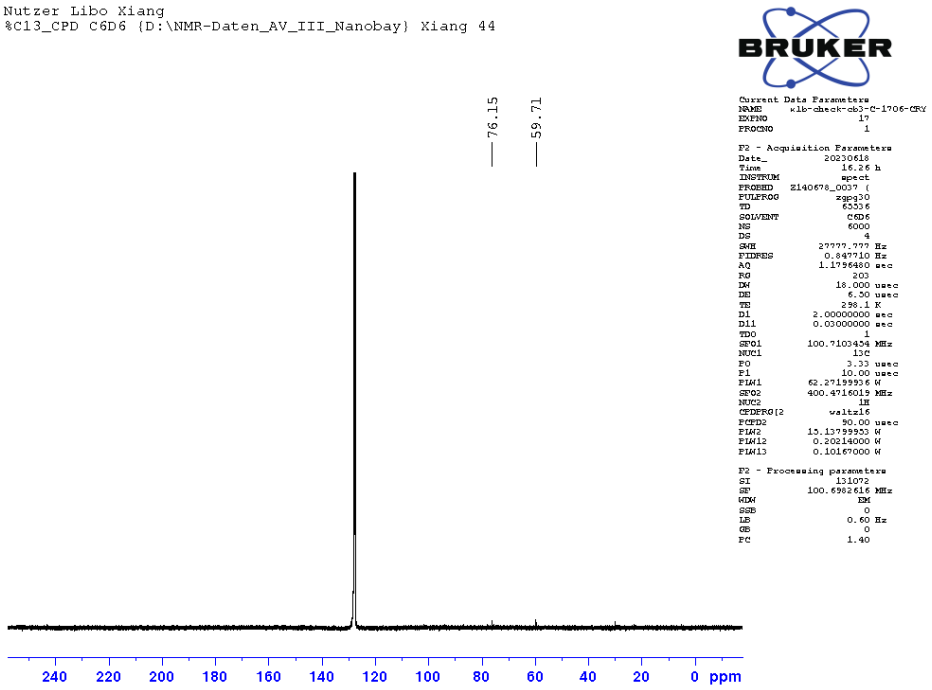

Figure S5. $^{13}C\{^{1}H\}$ NMR spectrum of **1** in C_6D_6 at 298 K.

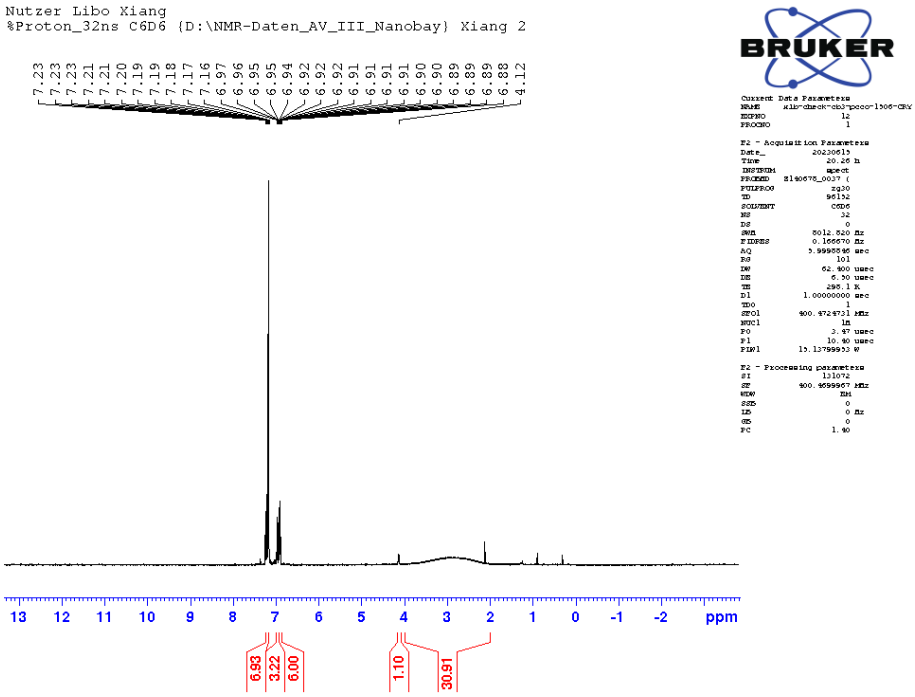

Figure S6. ^{1}H NMR spectrum of **3a** in C_6D_6 at 298 K.

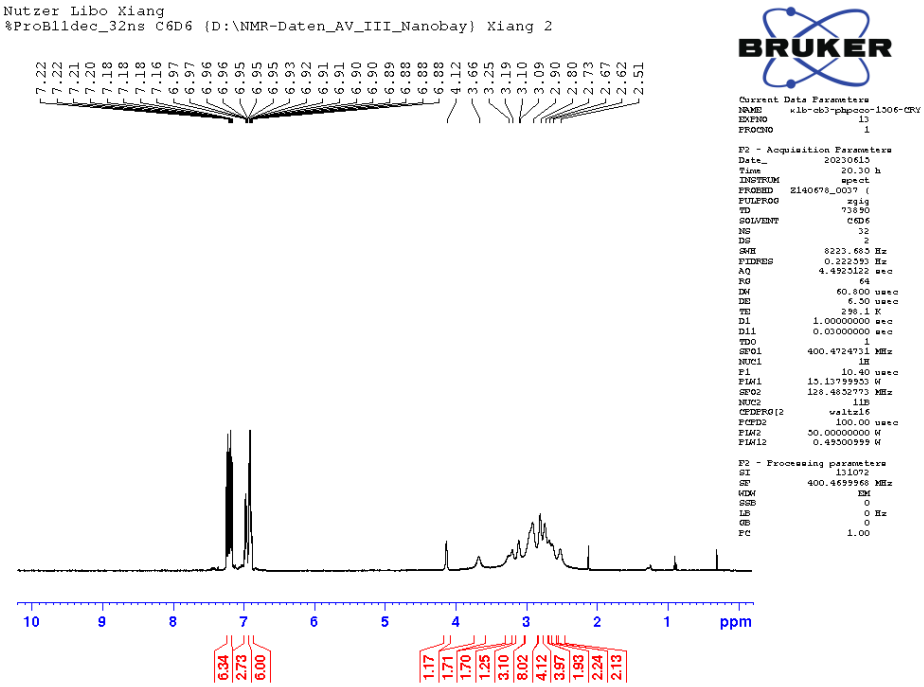

Figure S7. $^{1}H\{^{11}B\}$ NMR spectrum of **3a** in C_6D_6 at 298 K.

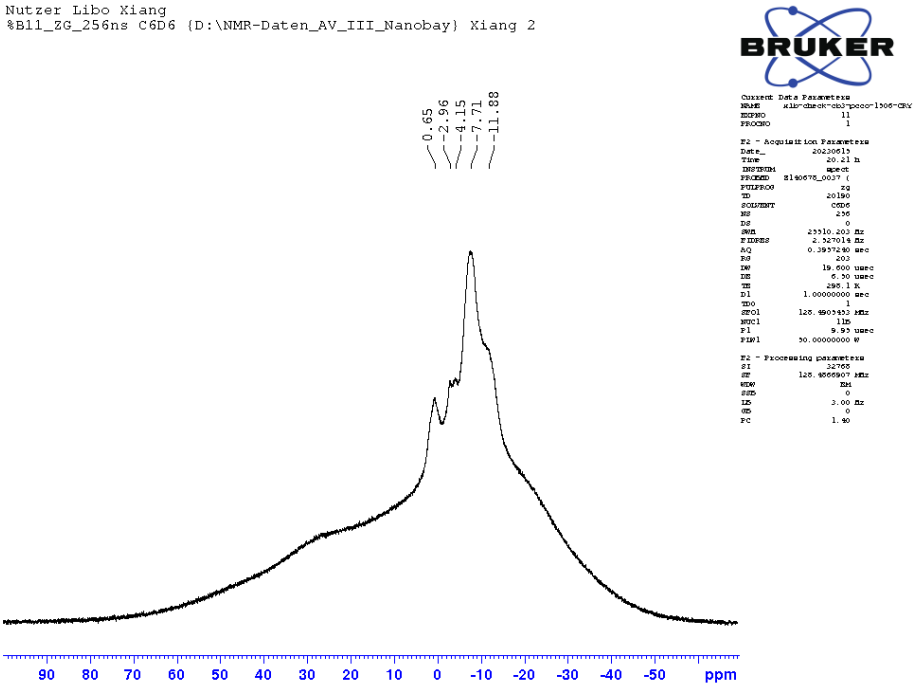

Figure S8. ^{11}B NMR spectrum of **3a** in C_6D_6 at 298 K.

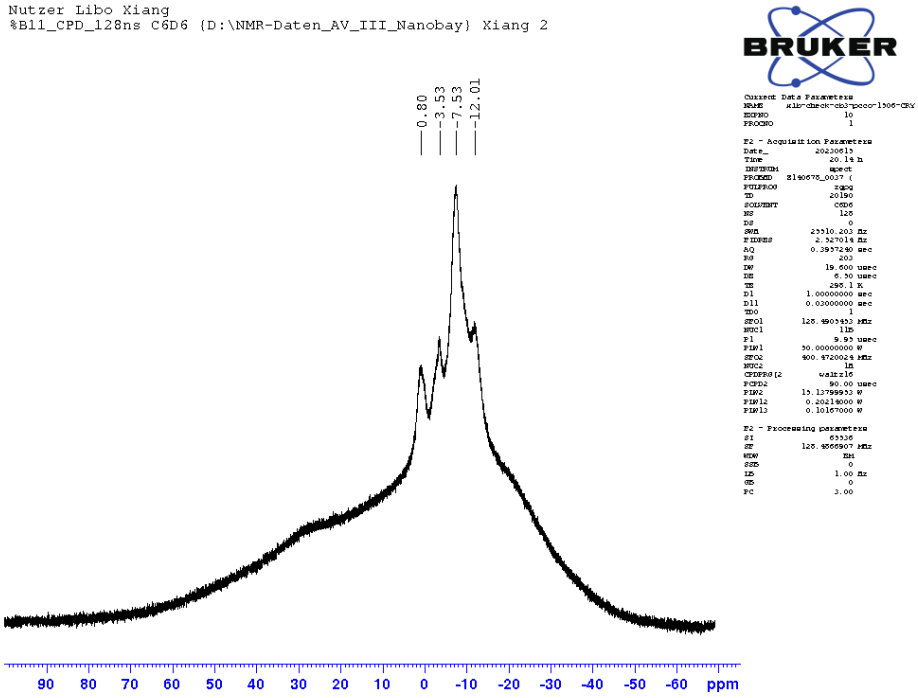

Figure S9. $^{11}B\{^{1}H\}$ NMR spectrum of **3a** in C_6D_6 at 298 K.

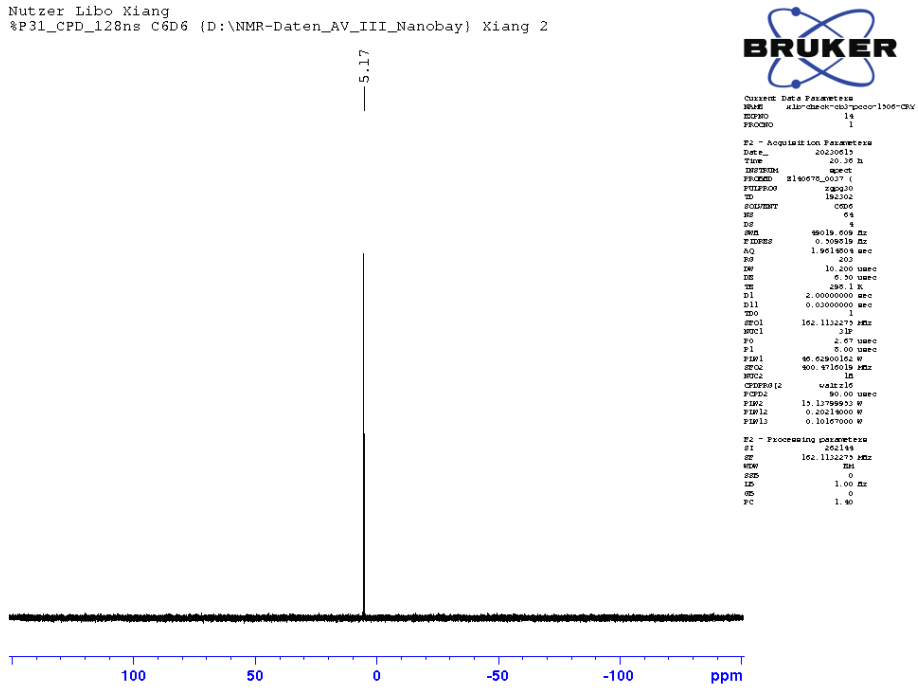

Figure S10. $^{31}P\{^{1}H\}$ NMR spectrum of **3a** in C_6D_6 at 298 K.

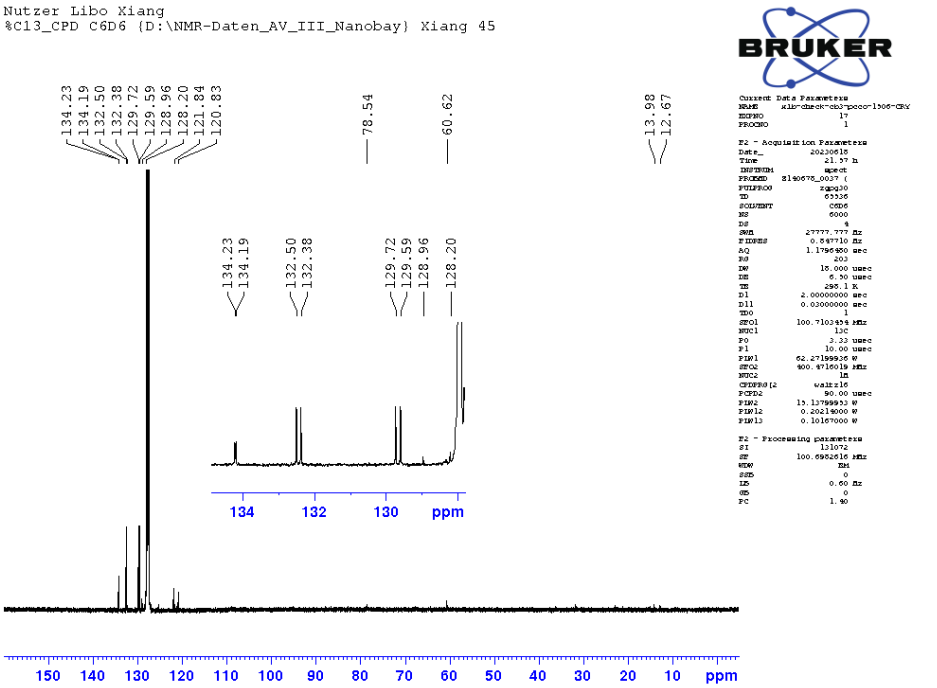

Figure S11. $^{13}C\{^{1}H\}$ NMR spectrum of **3a** in C_6D_6 at 298 K.

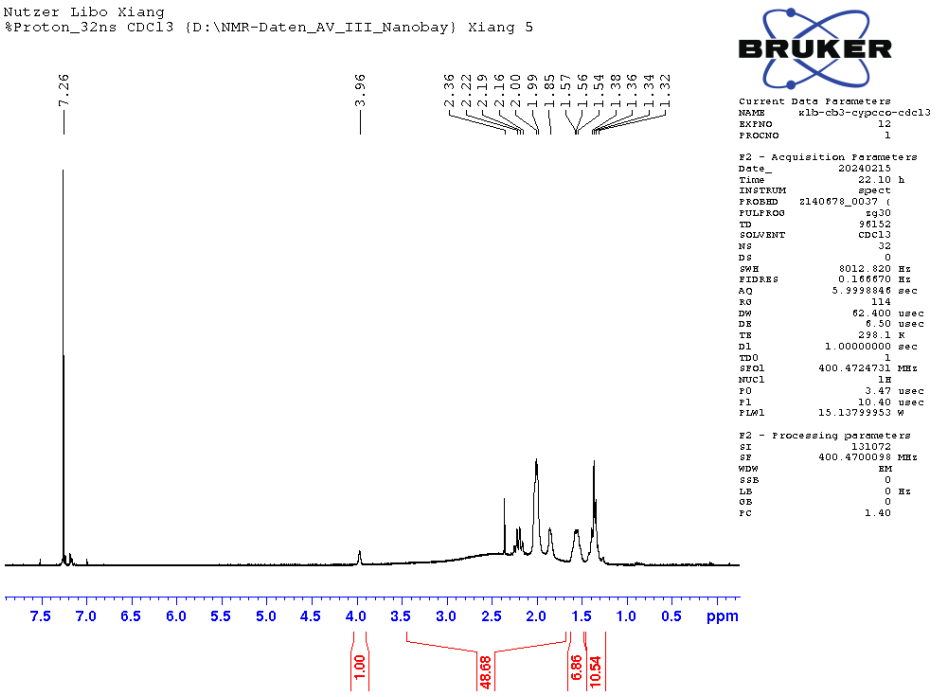

Figure S12. ^{1}H NMR spectrum of **3b** in $CDCl_3$ at 298 K.

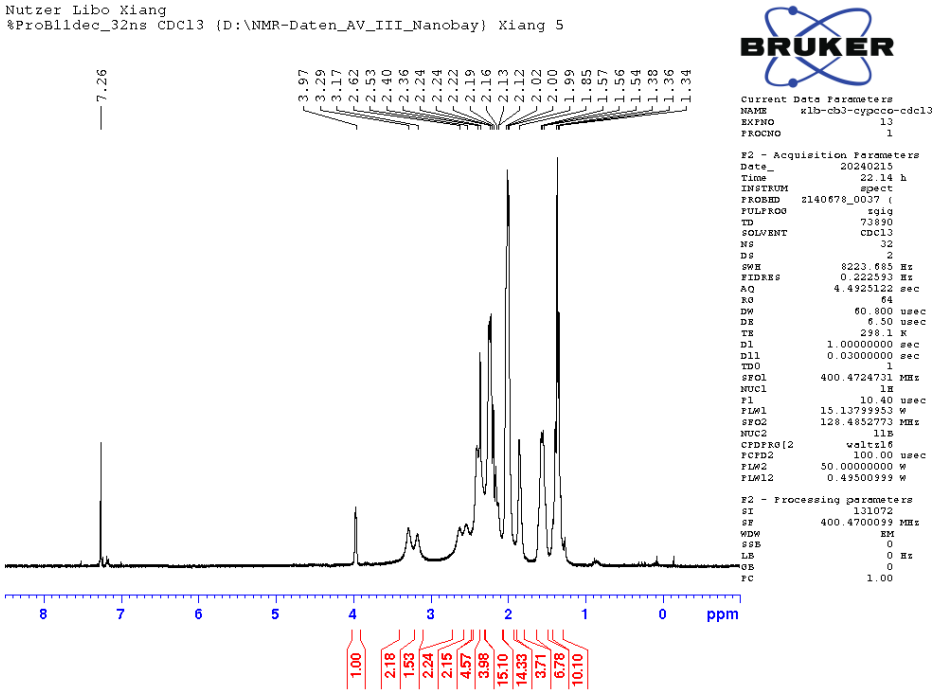

Figure S13. $^{1}H\{^{11}B\}$ NMR spectrum of **3b** in $CDCl_3$ at 298 K.

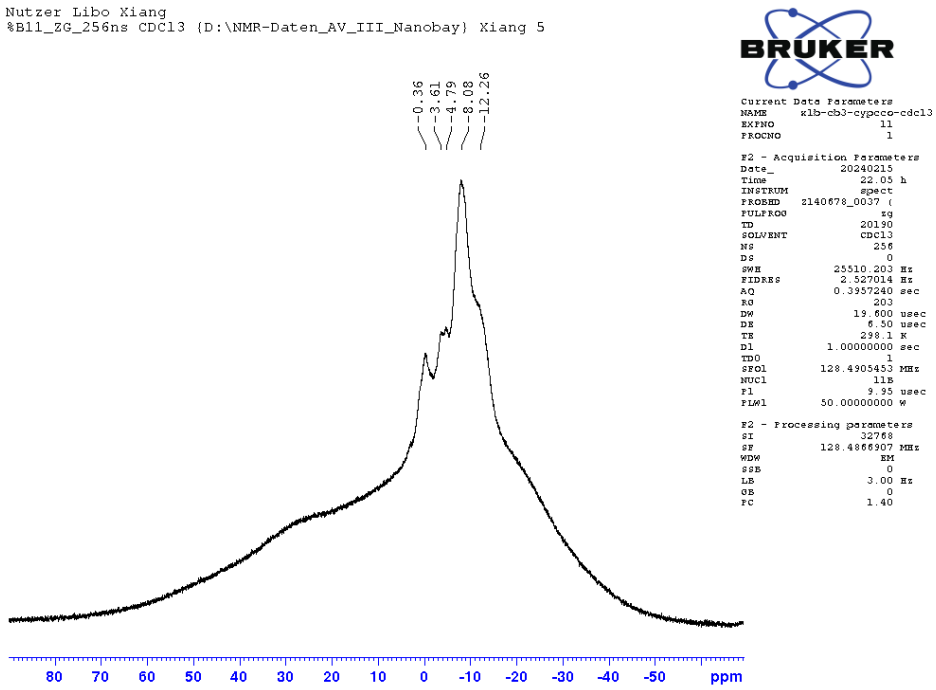

Figure S14. ^{11}B NMR spectrum of **3b** in $CDCl_3$ at 298 K.

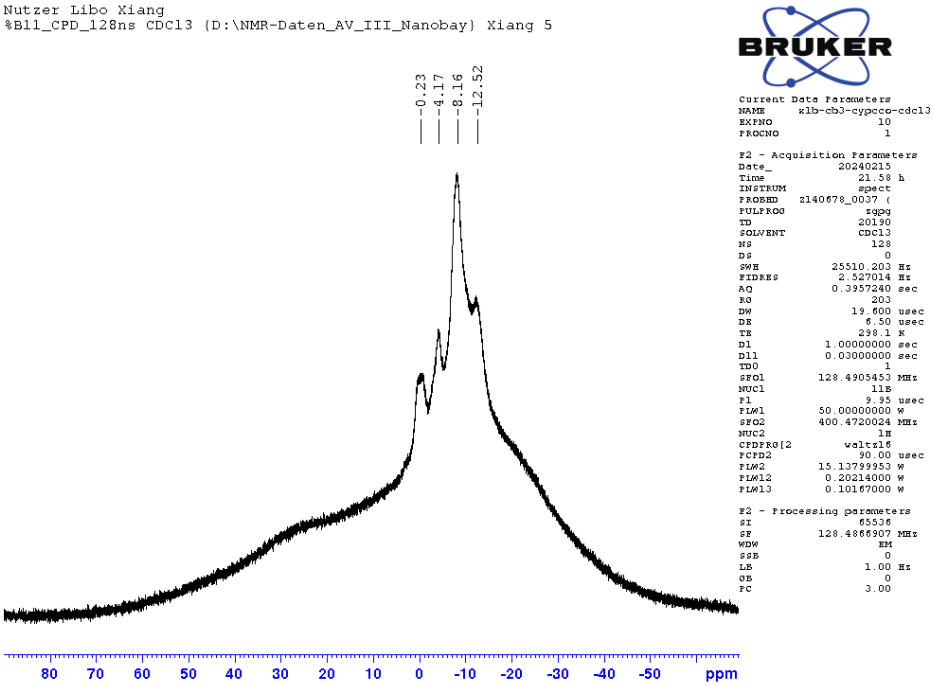

Figure S15. $^{11}B\{^1H\}$ NMR spectrum of **3b** in $CDCl_3$ at 298 K.

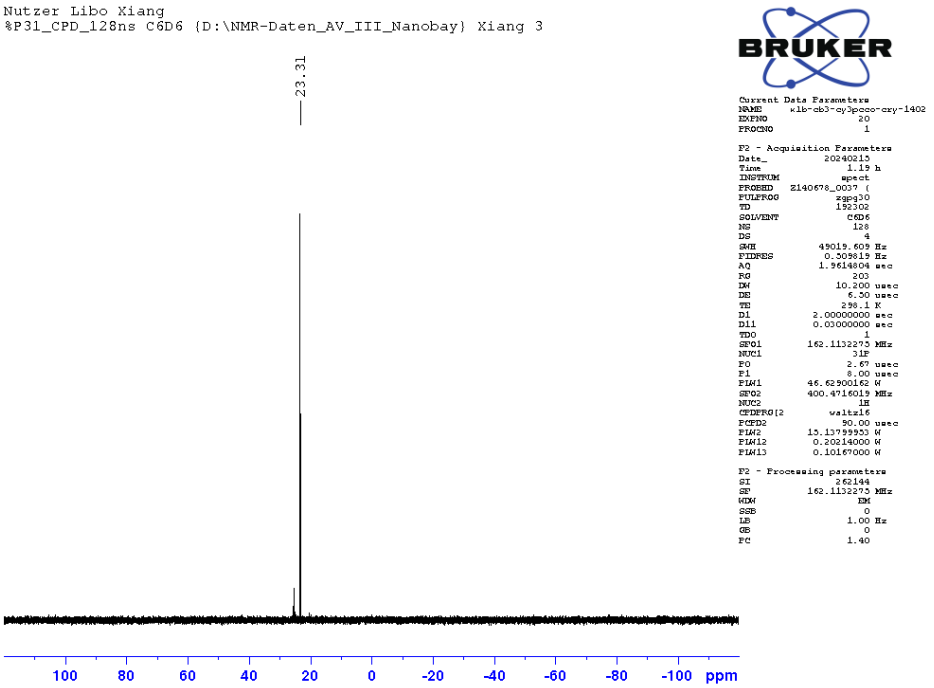

Figure S16. $^{31}P\{^1H\}$ NMR spectrum of **3b** in $CDCl_3$ at 298 K.

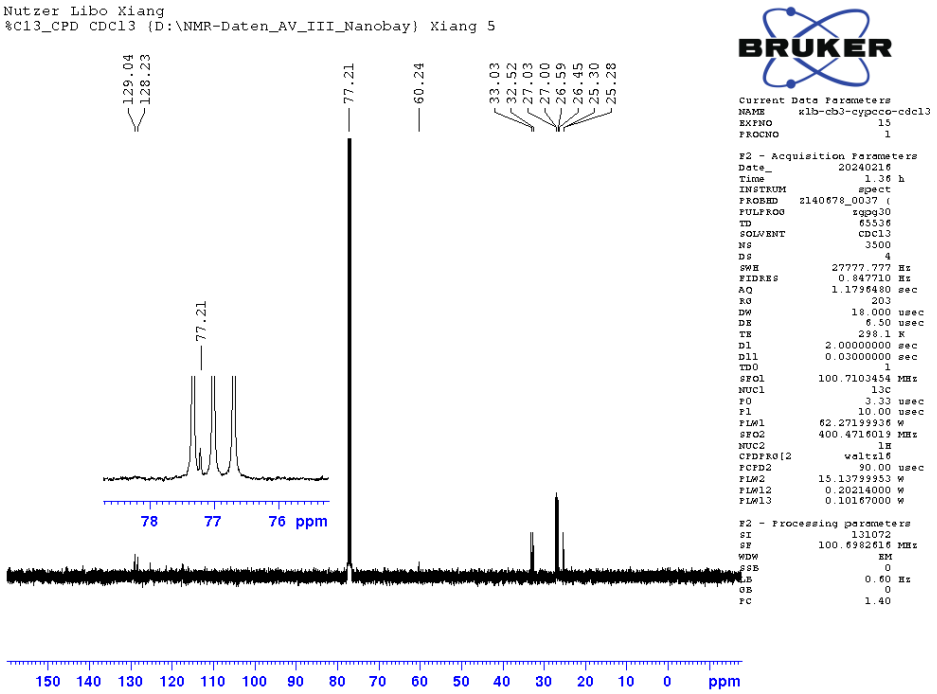

Figure S17. $^{13}C\{^{1}H\}$ NMR spectrum of **3b** in $CDCl_3$ at 298 K.

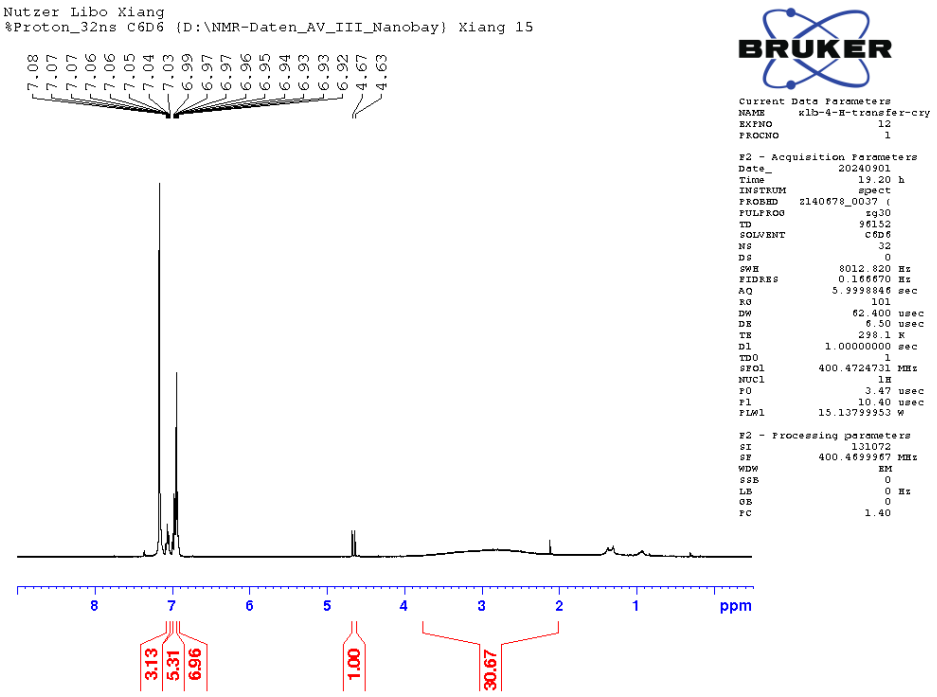

Figure S18. ^{1}H NMR spectrum of **4a** in C_6D_6 at 298 K.

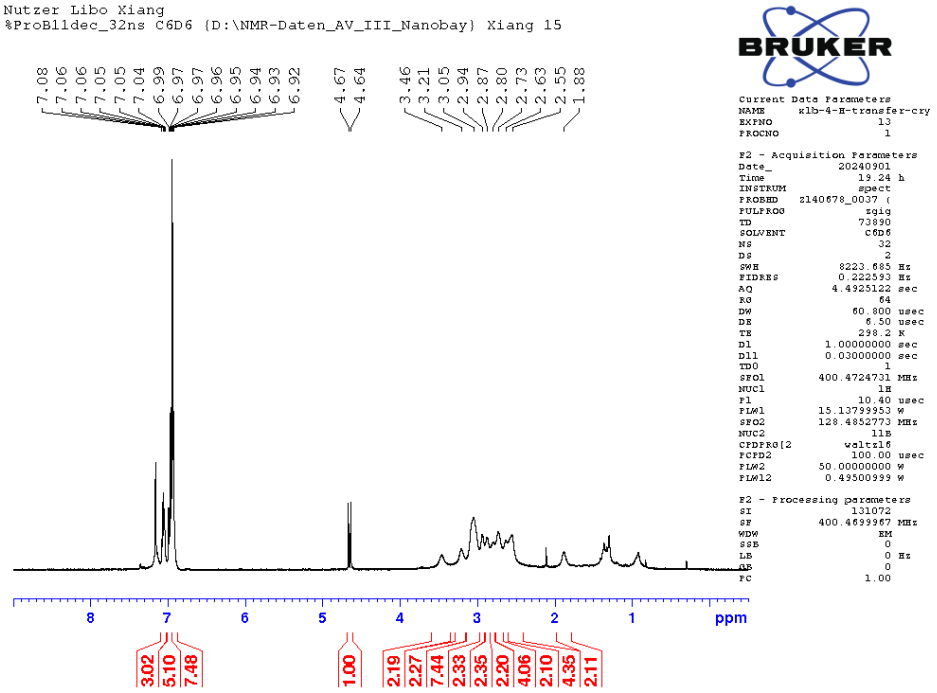

Figure S19. $^{1}H\{^{11}B\}$ NMR spectrum of **4a** in C_6D_6 at 298 K.

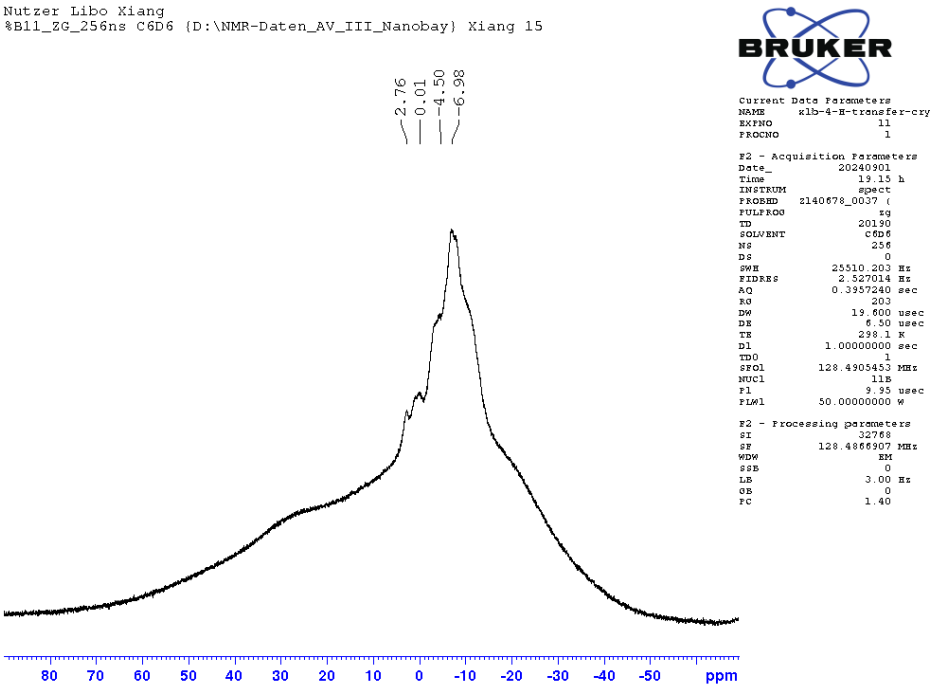

Figure S20. ^{11}B NMR spectrum of **4a** in C_6D_6 at 298 K.

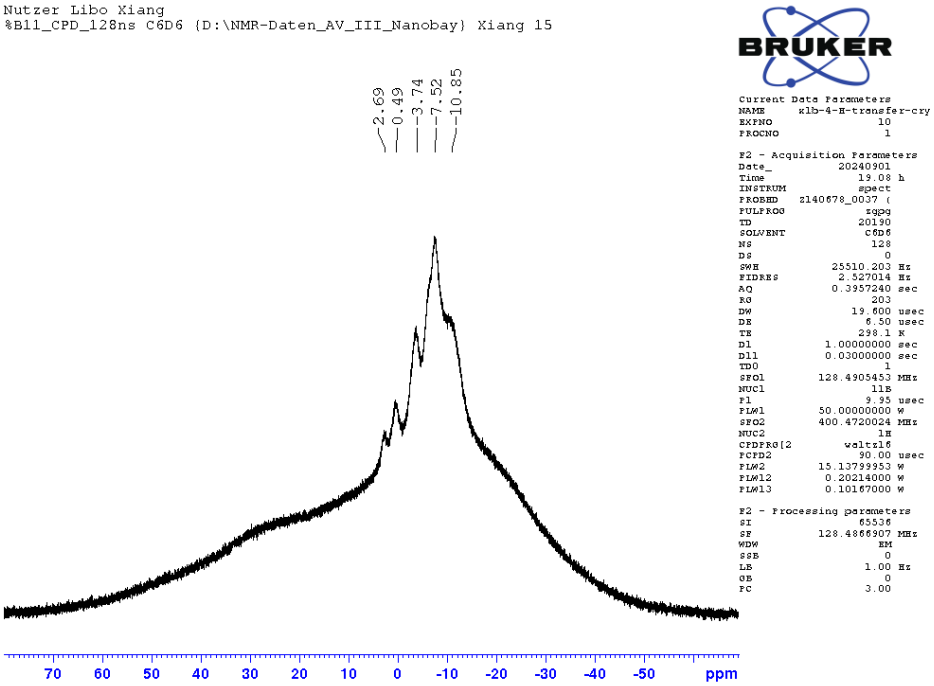

Figure S21. $^{11}B\{^{1}H\}$ NMR spectrum of **4a** in C_6D_6 at 298 K.

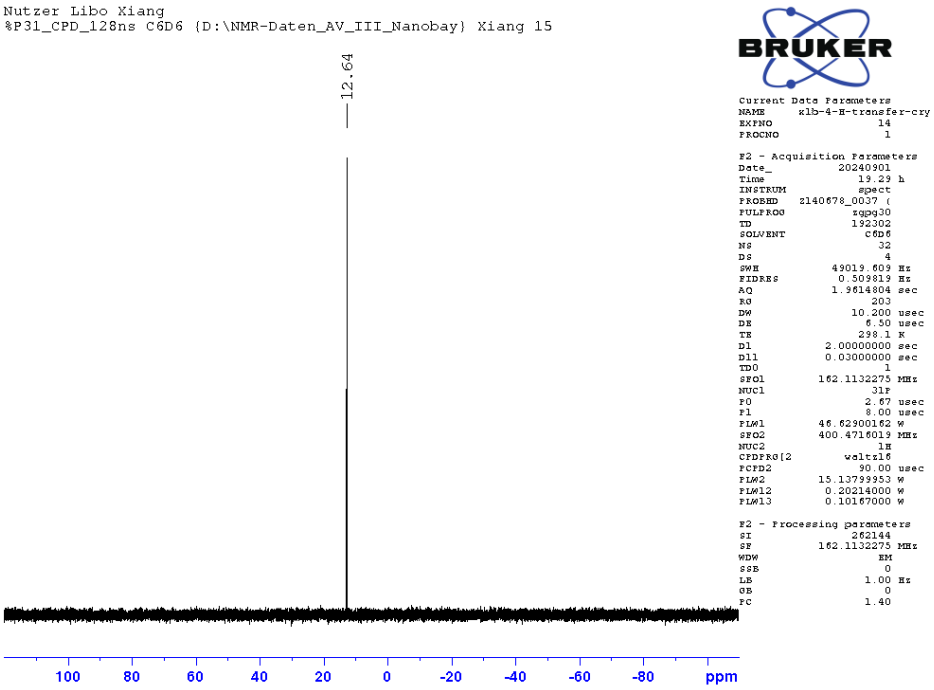

Figure S22. $^{31}P\{^{1}H\}$ NMR spectrum of **4a** in C_6D_6 at 298 K.

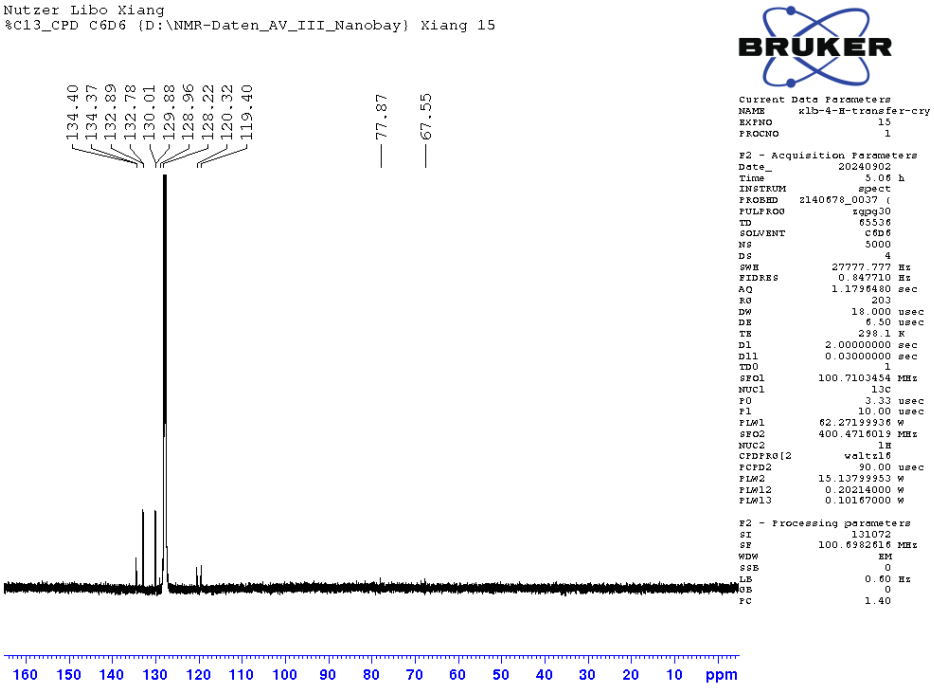

Figure S23. $^{13}C\{^{1}H\}$ NMR spectrum of **4a** in C_6D_6 at 298 K.

IR Spectroscopy

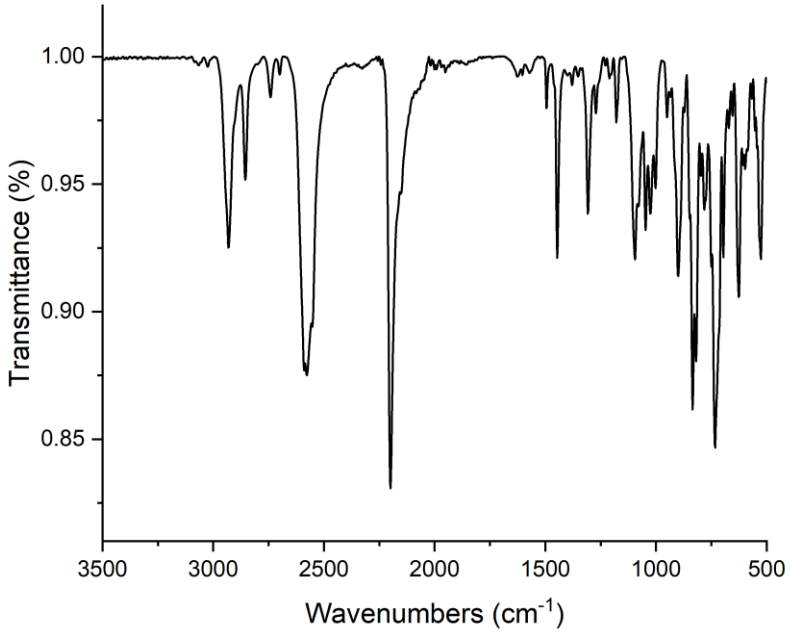

Figure S24. IR spectrum of **3a**.

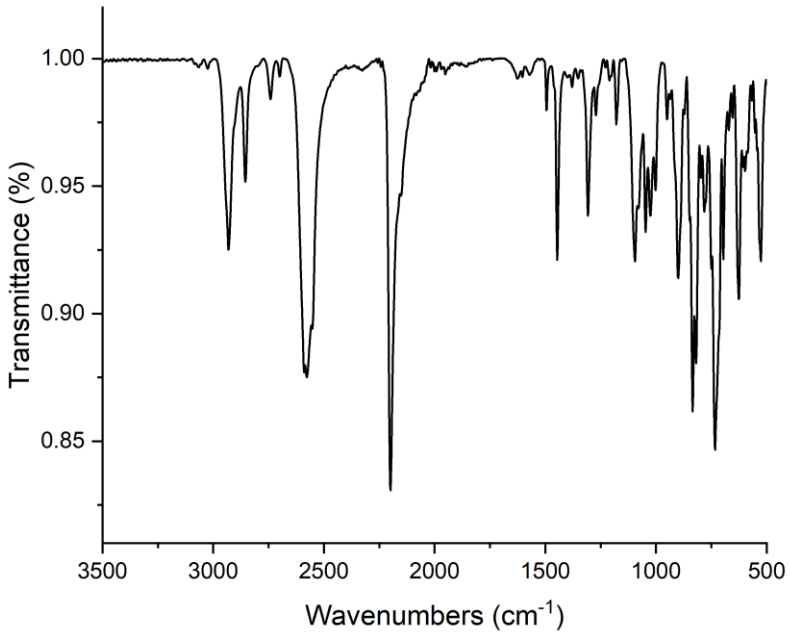

Figure S25. IR spectrum of **3b**.

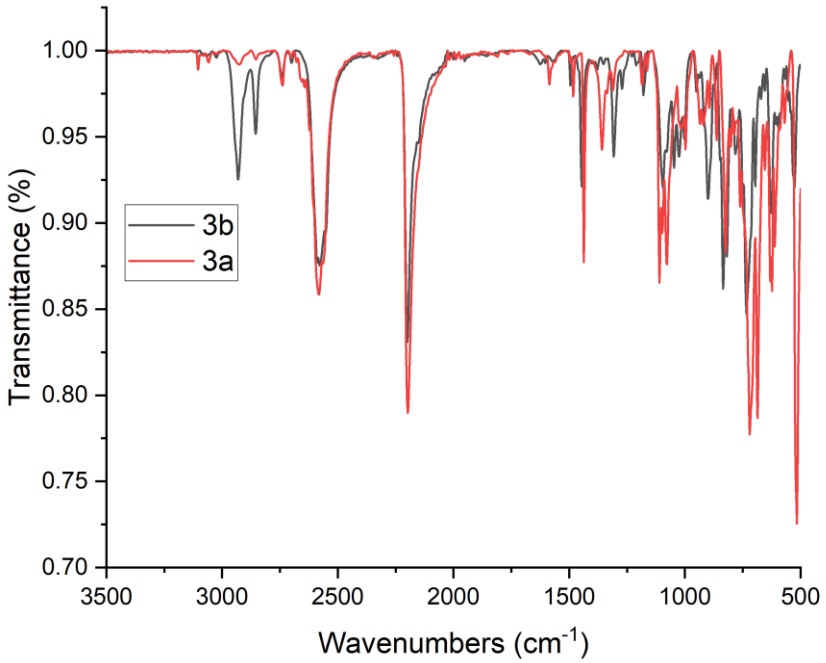

Figure S26. IR spectrum of **3a** and.**3b**

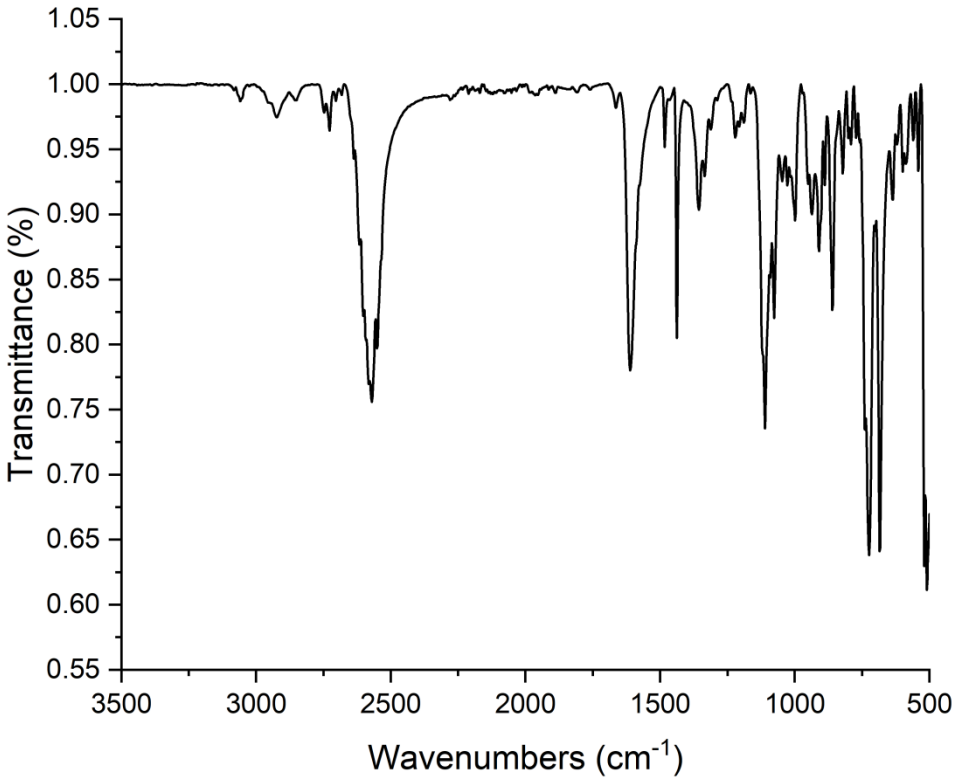

Figure S27. IR spectrum of **4a**.

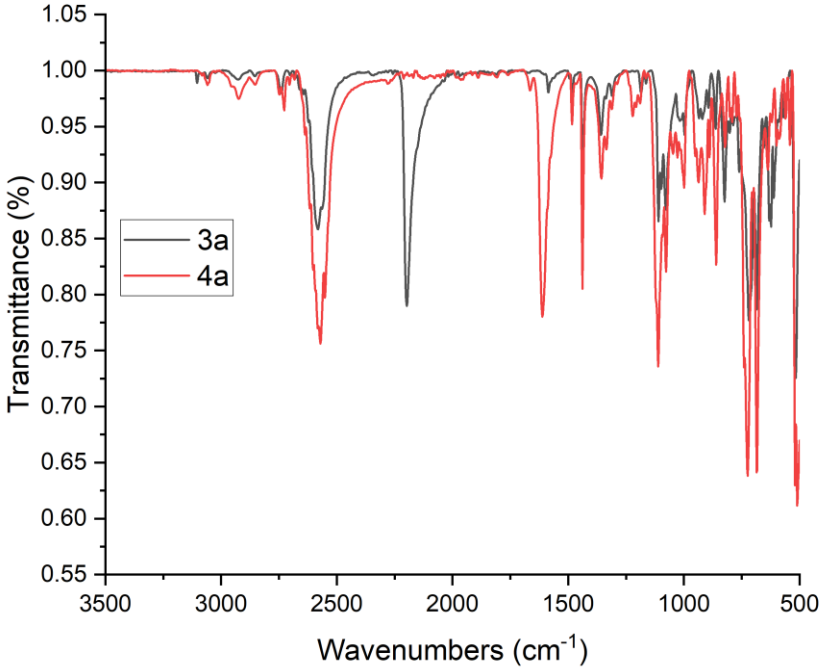

Figure S28. IR spectrum of **3a** and **4a**.

Characterizations of Lewis acidity

Gutmann–Beckett methods

Equimolar amount of Et_3PO was added to the C_6D_6 solution of **1**.

Table S1. Gutmann–Beckett method of **1**

Entry (in C_6D_6)	^{31}P NMR (δ)	Δδ (δsample-δTEPO)	Acceptor Numbers
Et_3PO	45.60		
1-Et_3PO	80.52	34.92	76.8

DFT calculation

All calculations were performed with the Gaussian 09 program.[4] All ground-state geometries were optimized using the B3LYP hybrid functional[5] in combination with def2-TZVP basis set.[6] Frequency calculations were performed to confirm that a local minimum has no imaginary frequency. For the FIA and HIA calculations, geometries and final electronic energies were obtained at the BP86-D3/def2-SVP level of theory.[7] The FIA reaction enthalpies were calculated according to the scheme proposed by Krossing using the given G3 anchor points and isodesmic reactions.[8] $\%V_{Bur}$ of values for the selected Lewis acids, obtained from the geometry of FIA adducts, were calculated using the SambVca 2.1 web application: https://www.molnac.unisa.it/OMtools/sambvca2.1/index.html.[9]

Table S2. FIA calculational data.

	E/Hartree	corr. Entha/ Hartree	E(H)/kJ mol^{-1}	FIA/kJ mol^{-1}	FIA/kJ mol^{-1} (ref. to SbF_5)
1	-1017.39	0.493927	-2669825.803	621.42	146.53
1-F^-	-1117.38	0.497998	-2932332.526		
A	-719.32	0.286094	-1887798.876	354.35	-120.53
A-F^-	-819.21	0.287503	-2150038.529		
B	-718.13	0.263823	-1884715.974	366.27	-108.62
B-F^-	-818.01	0.265238	-2146967.544		
C	-2206.67	0.180139	-5793060.606	452.68	-22.21
C-F^-	-2306.60	0.182442	-6055398.583		
D	-2007.17	0.172461	-5269288.298	456.67	-18.22
D-F^-	-2107.09	0.174809	-5531630.269		
E	-1018.59	0.516750	-2672918.865	581.53	106.64
E-F^-	-1118.57	0.520052	-2935385.692		

Table S3. HIA calculational data.

	E/Hartree	corr. Entha/ Hartree	E(H)/kJ mol^{-1}	FIA/kJ mol^{-1}	FIA/kJ mol^{-1} (ref. to $B(C_6F_5)_3$)
1	-1017.39	0.493927	-2669825.803	631.89	147.41
1-H^-	-1018.15	0.503462	-2671796.654		
A	-719.32	0.286094	-1887798.876	359.70	-124.78
A-H^-	-719.97	0.291212	-1889497.538		
B	-718.12	0.263823	-1884715.974	382.43	-102.04
B-H^-	-718.79	0.269972	-1886437.37		
C	-2206.67	0.180139	-5793060.606	484.47	0
C-H^-	-2207.38	0.18806	-5794884.043		
D	-2007.17	0.172461	-5269288.298	490.81	6.34
D-H^-	-2007.87	0.180164	-5271118.076		
E	-1018.59	0.516750	-2672918.865	602.45	117.98
E-H^-	-1019.34	0.525671	-2674860.28		

Table S4. Global Electrophilicity Index (GEI)[10] of compound **1** and **A** to **E**.

Compound	LUMO/eV	HOMO/eV	GEI/eV
1	-3.947	-8.865	4.17
A	-2.019	-6.883	2.04
B	-2.519	-6.098	2.59
C	-3.523	-7.651	3.78
D	-3.782	-7.236	4.39
E	-3.979	-8.986	4.20

Table S5. %V_{Bur} and pyramidization energy of compound **1** and **E**.

Compound	Anion	%V_{bur}	d(LA-F)/Å	Pyramidization energy/kJ•mol^{-1}	Steric Map
1	**1**-F$^-$	67.7	1.423	122.0	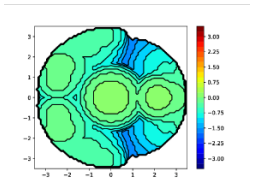
E	**E**-F$^-$	73.3	1.426	130.1	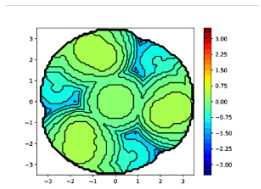

Crystallographic Details

The crystal data of **1** and **3a** was collected on a Bruker D8 VENTURE diffractometer with graphite monochromated $Mo_{K\alpha}$ radiation (λ = 0.71073 Å). Data reduction, scaling and absorption corrections were performed using SAINT (Bruker, V8.38A, 2013). The structure was solved with the XT structure solution program using the Intrinsic Phasing solution method[11] and by using Olex2[12] as the graphical interface. The model was refined with the ShelXL program[13] using Least Squares minimization. All non-hydrogen atoms were refined anisotropically. Hydrogen atoms were included in structure factor calculations. All hydrogen atoms were assigned to idealized geometric positions.

The crystal data of **3b** and **4a** were collected on a Rigaku XtaLAB Synergy-R diffractometer with a HPA area detector and multi-layer mirror monochromated Cu_{Ka} radiation. The structure was solved using intrinsic phasing method5, refined with the ShelXL program[13] and expanded using Fourier techniques.

Crystallographic data have been deposited with the Cambridge Crystallographic Data as supplementary publication nos. CCDC-2355581 (**1**), 2355582 (**3a**), 2355583 (**3b**), 2382930(**4a**). These data can be obtained free of charge from The Cambridge Crystallographic Data Centre via Data https://www.ccdc.cam.ac.uk

Details of the data collection and refinement for complexes **1**–**4a** are given in Table S6-S9.

Table S6. Crystal data and structure refinement for **1.**	
Identification code	1
Empirical formula	$C_6H_{31}B_{31}$
Formula weight	438.42
Temperature/K	100(2)
Crystal system	orthorhombic
Space group	*P*nma
a/Å	21.639(4)
b/Å	16.953(2)
c/Å	6.7994(12)
α/°	90
β/°	90
γ/°	90
Volume/Å^3	2494.3(7)
Z	4
ρ_{calc}g/cm^3	1.167
μ/mm^{-1}	0.047
F(000)	888.0
Crystal size/mm^3	0.444 × 0.32 × 0.251
Radiation	$Mo_{K\alpha}$ (λ = 0.71073)
2Θ range for data collection/°	3.764 to 52.728
Index ranges	-27 ≤ h ≤ 24, -18 ≤ k ≤ 21, -8 ≤ l ≤ 8
Reflections collected	27425
Independent reflections	2643 [R_{int} = 0.0574, R_{sigma} = 0.0280]
Data/restraints/parameters	2643/0/175
Goodness-of-fit on F^2	1.111
Final R indexes [I>=2σ (I)]	R_1 = 0.0615, wR_2 = 0.1808
Final R indexes [all data]	R_1 = 0.0678, wR_2 = 0.1869
Largest diff. peak/hole / e Å^{-3}	0.38/-0.57

Table S7. Crystal data and structure refinement for **3a.**	
Identification code	3a
Empirical formula	$C_{26}H_{46}B_{31}OP$
Formula weight	740.71
Temperature/K	100(2)
Crystal system	triclinic
Space group	*P*-1
a/Å	12.196(3)
b/Å	12.565(3)
c/Å	15.872(4)
α/°	91.154(8)
β/°	106.328(9)
γ/°	117.784(7)
Volume/Å^3	2032.1(9)
Z	2
ρ_{calc}g/cm^3	1.211
μ/mm^{-1}	0.096
F(000)	760.0
Crystal size/mm^3	0.34 × 0.236 × 0.116
Radiation	$Mo_{K\alpha}$ (λ = 0.71073)
2Θ range for data collection/°	3.724 to 53.462
Index ranges	-15 ≤ h ≤ 15, -15 ≤ k ≤ 15, -20 ≤ l ≤ 20
Reflections collected	68538
Independent reflections	8626 [R_{int} = 0.0623, R_{sigma} = 0.0340]
Data/restraints/parameters	8626/0/535
Goodness-of-fit on F^2	1.075
Final R indexes [I>=2σ (I)]	R_1 = 0.0498, wR_2 = 0.1258
Final R indexes [all data]	R_1 = 0.0562, wR_2 = 0.1300
Largest diff. peak/hole / e Å^{-3}	0.82/-0.26

Table S8. Crystal data and structure refinement for **3b**.	
Identification code	3b
Empirical formula	$C_{27}H_{64}B_{31}OP{\bullet}C_7H_8$
Formula weight	850.277
Temperature/K	100.15
Crystal system	triclinic
Space group	*P*-1
a/Å	10.9967(1)
b/Å	15.5241(2)
c/Å	15.9285(3)
α/°	69.719(1)
β/°	81.164(1)
γ/°	78.446(1)
Volume/Å^3	2488.44(6)
Z	2
ρ_{calc}g/cm^3	1.135
μ/mm^{-1}	0.678
F(000)	896.6
Crystal size/mm^3	0.14 × 0.11 × 0.09
Radiation	$Cu_{K\alpha}$ (λ = 1.54184)
2Θ range for data collection/°	5.94 to 150.28
Index ranges	-13 ≤ h ≤ 13, -19 ≤ k ≤ 17, -19 ≤ l ≤ 19
Reflections collected	45284
Independent reflections	9641 [R_{int} = 0.0300, R_{sigma} = 0.0170]
Data/restraints/parameters	9641/0/596
Goodness-of-fit on F^2	1.024
Final R indexes [I>=2σ (I)]	R_1 = 0.0703, wR_2 = 0.1808
Final R indexes [all data]	R_1 = 0.0722, wR_2 = 0.1814
Largest diff. peak/hole / e Å^{-3}	0.83/-0.44

Table S9. Crystal data and structure refinement for **4a**.	
Identification code	4a
Empirical formula	$C_{26}H_{46}B_{31}OP$
Formula weight	740.71
Temperature/K	100(2)
Crystal system	monoclinic
Space group	$P2_1/n$
a/Å	13.9904(2)
b/Å	17.1121(2)
c/Å	19.3321(2)
α/°	90
β/°	109.8020(10)
γ/°	90
Volume/Å^3	4354.53(10)
Z	4
ρ_{calc}g/cm^3	1.130
μ/mm^{-1}	0.720
F(000)	1520.0
Crystal size/mm^3	0.3 × 0.25 × 0.12
Radiation	$Cu_{K\alpha}$ (λ = 1.54184)
2Θ range for data collection/°	6.826 to 146.206
Index ranges	-17 ≤ h ≤ 17, -19 ≤ k ≤ 21, -23 ≤ l ≤ 21
Reflections collected	42906
Independent reflections	8374 [Rint = 0.0204, Rsigma = 0.0168]
Data/restraints/parameters	8374/0/532
Goodness-of-fit on F^2	1.036
Final R indexes [I>=2σ (I)]	R_1 = 0.0381, wR_2 = 0.1018
Final R indexes [all data]	R_1 = 0.0401, wR_2 = 0.1032
Largest diff. peak/hole / e Å^{-3}	0.34/-0.29

Reference

1 A. Brar, D. K. Unruh, A. J. Aquino, C. Krempner, *Chem. Commun.* **2019**, *55*, 3513-3516.

2 F. A. Gomez, M. F. Hawthorne, *J. Org. Chem.* **1992**, *57*, 1384-1390.

3 (a) C. Zhang, J. Wang, Z. Lin, Q. Ye, *Inorg. Chem.* **2022**, *61*, 18275–18284; (b) Ryan, S. J.; Schimler, S. D.; Bland, D. C.; Sanford, M. S. Org. Lett. **2015**, *17*, 1866-1869.

4 M. J. Frisch, G. W. Trucks, H. B. Schlegel, G. E. Scuseria, M. A. Robb, J. R. Cheeseman, G. Scalmani, V. Barone, B. Mennucci, G. A. Petersson, H. Nakatsuji, M. Caricato, X. Li, H. P. Hratchian, A. F. Izmaylov, J. Bloino, G. Zheng, J. L. Sonnenberg, M. Hada, M. Ehara, K. Toyota, R. Fukuda, J. Hasegawa, M. Ishida, T. Nakajima, Y. Honda, O. Kitao, H. Nakai, T. Vreven, J. A., Jr. Montgomery, J. E. Peralta, F. Ogliaro, M. Bearpark, J. J. Heyd, E. Brothers, K. N. Kudin, V. N. Staroverov, R. Kobayashi, J. Normand, K. Raghavachari, A. Rendell, J. C. Burant, S. S. Iyengar, J. Tomasi, M. Cossi, N. Rega, N. J. Millam, M. Klene, J. E. Knox, J. B. Cross, V. Bakken, C. Adamo, J. Jaramillo, R. Gomperts, R. E. Stratmann, O. Yazyev, A. J. Austin, R. Cammi, C. Pomelli, J. W. Ochterski, R. L. Martin, K. Morokuma, V. G. Zakrzewski, G. A. Voth, P. Salvador, J. J. Dannenberg, S. Dapprich, A. D. Daniels, Ö. Farkas, J. B. Foresman, J. V. Ortiz, J. Cioslowski, D. J. Fox, Gaussian 09, Revision D.01; Gaussian, Inc.: Wallingford CT, **2013**.

5 A. D. J. Becke, *Chem. Phys.* **1993**, *98*, 5648−5652.

6 P. J. Stephens, F. J. Devlin, C. F. Chabalowski, M. J. J. Frisch, *Phys. Chem.* **1994**, *98*, 11623−11627.

7 a) J. P. Perdew, *Phys. Rev. B* **1986**, *33*, 8822–8824; b) A. D. Becke, *Phys. Rev. A* **1988**, *38*, 3098–3100; c) S. Grimme, S. Ehrlich, L. Goerigk, *J. Comput. Chem.* **2011**, *32*, 1456–1465; d) E. R. Johnson, A. D. Becke, *J. Chem. Phys.* **2005**, *123*, 24101; e) S. Grimme, J. Antony, S. Ehrlich, H. Krieg, *J. Chem. Phys.* **2010**, *132*, 154104; f) A. D. Becke, E. R. Johnson, *J. Chem. Phys.* **2005**, *122*, 154104.

8 a) H. Böhrer, N. Trapp, D. Himmel, M. Schleep, I. Krossing, *Dalton Trans.* **2015**, *44*, 7489–7499; b) L. Greb, *Chem. Eur. J.* **2018**, *24*, 17881–17896; c) L. O. Müller, D. Himmel, J. Stauffer, G. Steinfeld, J. Slattery, G. Santiso-Quiñones, V. Brecht, I. Krossing, *Angew. Chem. Int. Ed.* **2008**, *47*, 7659–7663.

9 a) A. C. Hillier, W. J. Sommer, B. S. Yong, J. L. Petersen, L. Cavallo, S. P. Nolan, *Organometallics*, **2003**, *22*, 4322-4326; b) A. Poater, F. Ragone, S. Giudice, C. Costabile, R. Dorta, S. P. Nolan, L. Cavallo, *Organometallics*, **2008**, *27*, 2679-2681; (d) S. Díez-González and S. P. Nolan, *Coord. Chem. Rev.*, **2007**, *251*, 874-883; (e) A. Gómez-Suárez, D. J. Nelson and S. P. Nolan, *Chem. Commun.*, **2017**, *53*, 2650-2660.

10 a) P. Pérez, L. R. Domingo, A. Aizman, R. Contreras, *Theor. Comput. Chem.* **2007**, *19*, 139-201; b) A. R. Jupp, T. C. Johnstone, D. W. Stephan, *Inorg. Chem.* **2018**, *57*, 14764−14771.

11 G. M. Sheldrick, SHELXT - Integrated space-group and crystal-structure determination. *Acta Cryst. A* **2015**, *71*, 3-8.

12 O. V. Dolomanov, L. J. Bourhis, R. J. Gildea, J. A. K. Howard, H. Puschmann, OLEX2: a complete structure solution, refinement and analysis program. *J. Appl. Cryst.* **2009**, *42*, 339–341.

13 G. M. Sheldrick, A short history of SHELX. *Acta Cryst. A* **2008**, *64*, 112-122.